

## Electrical resistivity and magnetic susceptibility in the amorphous $\text{Cr}_x\text{Ge}_{1-x}$ alloy system

T. Sato, A. Jono,\* E. Ohta, and M. Sakata

*Department of Instrumentation Engineering, Faculty of Science and Technology, Keio University, 3-14-1 Hiyoshi, Kohoku-ku, Yokohama-shi, Kanagawa 223, Japan*

(Received 29 February 1988; revised manuscript received 23 June 1988)

The electrical resistivity and magnetic susceptibility of amorphous  $\text{Cr}_x\text{Ge}_{1-x}$  alloys ( $0 \leq x \leq 0.65$ ) prepared by means of the flash-evaporation method were investigated in relation to the amorphous structure. The partial pair distribution function determined by the x-ray diffraction method shows a change from the tetrahedral random network to the dense-random-packing structure with increasing Cr content. The electrical resistivity shows a transition from semiconductorlike conduction to metal-like conduction in accordance with the structure change. On the basis of the idea of Mott's hopping conduction, the density of states at the Fermi level increases with increasing Cr content and the length of decay of a localized wave function decreases with decreasing substrate temperature during evaporation. An increase in the Fermi level was deduced from analysis of the metallic conduction in terms of the Baym-Faber-Ziman theory incorporating electron mean-free-path effects. The magnetic susceptibility shows the Curie-Weiss-like behavior characterized by a significantly small localized moment per Cr atom ( $\mu_{\text{eff}} \sim 0.4\mu_B$ ). The small moment is discussed on the basis of the idea of the virtual bound state, with local environment effects taken into account.

### I. INTRODUCTION

The magnetic moment of a transition-metal atom in a disordered matrix often shows an intrinsically different nature from that in the corresponding ordered matrix. Several groups have proposed mechanisms for the occurrence of the different nature of the magnetic moments by comparing magnetic properties of amorphous alloys containing transition-metal atoms with those of the crystalline materials, and indicated an influence of host disorder in favor of local moment formation on a transition-metal atom.<sup>1-11</sup> From these studies of the magnetic properties of amorphous alloys prepared under various conditions, the significance of local environment effects on the local moment formation has been suggested. Electrical resistivity of amorphous alloys containing transition metal atoms has also been studied experimentally and theoretically by many groups. The temperature dependence of the electrical resistivity is mainly characterized by the structure factor and the mean free path of conduction electrons.<sup>12,13</sup> These contents suggest a significance of the systematic and comprehensive study of the atomic structure and electrical and magnetic properties to make clear the nature of amorphous alloys, especially those containing transition metal atoms.

In the study of the crystalline Cr-Ge system, work on five intermetallic compounds ( $\text{Cr}_3\text{Ge}$ ,  $\text{Cr}_5\text{Ge}_3$ ,  $\text{Cr}_{11}\text{Ge}_8$ ,  $\text{CrGe}$ , and  $\text{Cr}_{11}\text{Ge}_{19}$ ) has been reported,<sup>14-25</sup> and an increase in the Cr-Cr atomic distance with increasing Ge content results in an increase in the degree of electron correlation.<sup>24,25</sup> In particular, their magnetic properties are characterized by itinerant electrons with weak interaction except for ferromagnetic  $\text{Cr}_{11}\text{Ge}_{19}$ .<sup>24,25</sup> Furthermore, we claimed that  $\text{Cr}_{11}\text{Ge}_8$  and  $\text{CrGe}$  are nearly ferromagnetic metals for which spin-fluctuation effects play a significant role.<sup>25</sup> On the other hand, work on amorphous Cr-Ge alloys has been reported over a wide

composition range,<sup>7,26</sup> because they contain a glass-former atom, Ge. We have made the amorphous structure analysis with electron diffraction and the measurements of electrical resistivity and magnetic susceptibility on several samples of the amorphous Cr-Ge alloys prepared by means of vapor quenching method, and the following results have been obtained.<sup>7</sup>

(1) Amorphous structure is verified for  $\text{Cr}_x\text{Ge}_{1-x}$  with  $x \leq 0.65$ .

(2) As the Cr content increases, the structure changes from the tetrahedral random network to the dense random packing.

(3) The electrical resistivity shows semiconductorlike behavior for lower Cr concentration and metal-like behavior for higher Cr concentration, which corresponds to a change in the structure.

(4) The magnetic susceptibility shows Curie-Weiss behavior, suggesting a local moment formation on Cr atoms, but the value of moment per Cr atom is evaluated as an extraordinarily small one. These results suggest a significant correlation between spatial structure and electrical resistivity, and a substantial change in magnetic moment on Cr atoms with amorphization. Therefore, we feel an interest in a comprehensive study of the amorphous nature of the amorphous Cr-Ge alloys in comparison with the crystalline Cr-Ge intermetallic compounds.

In the present paper, amorphous Cr-Ge alloys were prepared by the flash evaporation method, and the partial pair distribution functions are determined by the x-ray diffraction method. Detailed measurements of electrical resistivity and magnetic susceptibility were made in the temperature range from 4.2 to 300 K, and the correlation between the data and atomic structure is discussed. Furthermore, the electrical resistivity is also measured on the samples prepared at low substrate temperature to investigate a change in the amorphous nature with different preparation conditions. We give a comprehensive discus-

sion of the random structure effect on the electrical and magnetic properties of the amorphous Cr-Ge alloys at last.

## II. EXPERIMENTAL METHOD

### A. Sample preparation

High-purity Cr (99.99% purity) and Ge (99.999% purity) powders were mixed in the desired compositions and melted at 1190°C in evacuated quartz tubes and then quenched in water. The product was crushed, and the  $\text{Cr}_x\text{Ge}_{1-x}$  alloys were deposited by flash evaporation method onto glass substrates covered with collodion films. The substrate temperature was held at room temperature and the pressure was  $1 \times 10^{-5}$  Torr during evaporation. The  $\text{Cr}_x\text{Ge}_{1-x}$  film was removed in acetone and then dried. The flake samples were used for the structure analysis by x-ray diffraction method and the magnetic measurements. On the other hand, the sample for electrical resistivity measurements was also prepared by flash evaporation method onto glass substrates whose substrate temperatures  $T_D$  were room temperature and 130 K. The film thickness was determined by multiple-beam interferometry and ranged from 2000 to 10000 Å for x-ray diffraction and magnetic measurements and from 200 to 3000 Å for electrical resistivity measurements. Composition of the film was determined by means of electron probe microanalysis. Since the analyzed Cr concentration of the film tends to be lower than that of the vapor source within 5 at. % as shown in Fig. 1, we will use the analyzed value as sample composition. We also verified no gross inhomogeneities in Cr composition in a single sample by making composition analysis on several portions of the same sample.

### B. Structure analysis

The amorphous Cr-Ge samples prepared at room temperature were plated onto  $(100)4^\circ \pm 1^\circ$  wafers. X-ray scattering intensity was measured at room temperature

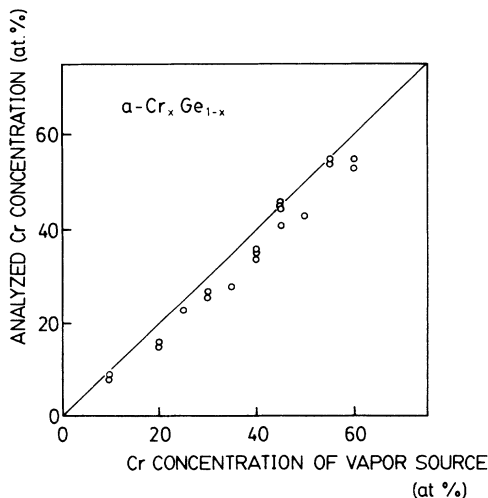


FIG. 1. Analyzed Cr concentration of amorphous Cr-Ge alloys against that of vapor source.

with three radiations of Mo, Cu, and Fe  $K\alpha$  using the step scan mode of operation. The data were analyzed on the basis of the method by Waseda and Tamaki.<sup>27</sup> The total structure factors  $S(K)$  were obtained in the reciprocal-space region  $0.7 \text{ \AA}^{-1} \leq K \leq 6.0 \text{ \AA}^{-1}$  using the atomic scattering factors and the anomalous dispersion terms calculated by Cromer and Waber,<sup>28</sup> and Cromer,<sup>29</sup> respectively. On the basis of values of  $S(K)$ , the partial structure factors  $S_{ij}$  ( $i, j = \text{Cr or Ge}$ ) were extracted by selecting a set of  $S_{ij}(K)$  for a fixed value of  $K$  in the range of allowed structure factors proposed by Edwards *et al.*<sup>30</sup> so as to minimize error between  $S(K)$  obtained above and the calculated one from a set of  $S_{ij}(K)$ . The partial pair distribution functions  $G_{ij}(r)$  were calculated using the resultant  $S_{ij}(K)$  with 0.06 for  $a$  in the artificial temperature factor  $\exp(-aK^2)$ .

### C. Electrical and magnetic measurements

The electrical resistivity  $\rho$  was measured for several samples of the amorphous Cr-Ge thin films deposited at room temperature and 130 K using the conventional dc four-terminal method. The error of the value of  $\rho$  is about 10% due to error in the measurement of film thickness by multiple interferometry. The magnetization  $\sigma$  and the magnetic susceptibility  $\chi$  were measured for the amorphous flakes of Cr-Ge alloys prepared at room temperature using a pendulum magnetic balance. The magnetic susceptibility  $\chi$  was measured at temperatures between 4.2 and 300 K in the magnetic field  $H = 6.3$  kOe. The accuracy of absolute value of the measured magnetization was about 2%, limited by deviations of the sample position. On the other hand, the accuracy of the absolute value of magnetic susceptibility was typically 4% owing to error in measurement of magnetic field.

## III. EXPERIMENTAL RESULTS

### A. Structure analysis

There is no sharp x-ray diffraction line for the  $\text{Cr}_x\text{Ge}_{1-x}$  sample prepared at room temperature with  $x \leq 0.65$ , which corresponds to its amorphous structure. Figure 2 shows the total structure factor  $S(K)$  for several samples of the amorphous  $\text{Cr}_x\text{Ge}_{1-x}$  alloys using radiation of Cu  $K\alpha$ . Here, we note that zero of  $S(K)$  for each  $\text{Cr}_x\text{Ge}_{1-x}$  alloy corresponds to  $100x$  in Fig. 2. The intensity of the first peak of pure amorphous Ge becomes remarkably small with shifting of its position in the direction of large  $K$  as Cr content increases, and disappears for  $x = 0.55$ . On the other hand, the second peak of pure amorphous Ge shifts in the opposite direction. The second peak splitting can be observed for  $x = 0.27$ . This feature is similar to that observed for the structure factors obtained by the electron diffraction method.<sup>7</sup>

Figure 3 shows the partial pair distribution functions  $G_{ij}(r)$  extracted from  $S(K)$ , where zero of  $G_{ij}(r)$  is also designated in the same way as in Fig. 2. The peak in  $G_{\text{CrCr}}(r)$  centered at  $\sim 3.5 \text{ \AA}$  shifts in the direction of small  $r$  with increasing Cr content. For  $x \geq 0.36$  the other peak appears at  $\sim 2 \text{ \AA}$ . There are peaks centered at

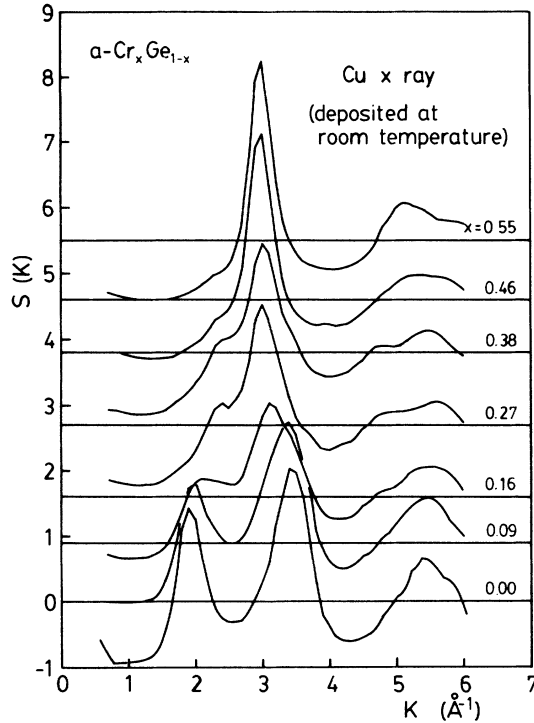


FIG. 2. Total structure factor  $S(K)$  of amorphous  $\text{Cr}_x\text{Ge}_{1-x}$  prepared at room temperature for  $x=0, 0.09, 0.16, 0.27, 0.38, 0.46,$  and  $0.55$  using radiation of  $\text{Cu } K\alpha$ . The zero of  $S(K)$  for each sample corresponds to  $100x$ .

$\sim 2.5 \text{ \AA}$  and  $\sim 4 \text{ \AA}$  in  $G_{\text{CrGe}}(r)$ , where the intensity of first and second peaks increases and decreases with increasing Cr content, respectively. The position and intensity of the first peak in  $G_{\text{GeGe}}(r)$  scarcely change, while the intensity of the second peak decreases and then increases with increasing Cr content. For  $x \leq 0.27$  the first peak in  $G_{\text{CrCr}}(r)$  locates at larger  $r$  in comparison with those in  $G_{\text{CrGe}}(r)$  and  $G_{\text{GeGe}}(r)$ , while the opposite relation is observed for  $x > 0.27$ , which suggests a change in the nearest-neighbor atom pair.

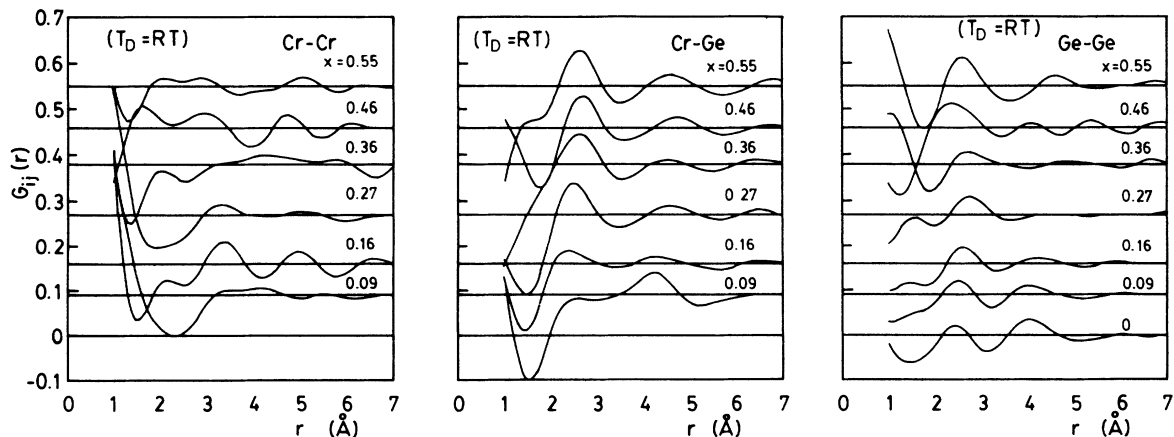


FIG. 3. Partial pair distribution functions  $G_{ij}(r)$  ( $i, j = \text{Cr or Ge}$ ) of amorphous  $\text{Cr}_x\text{Ge}_{1-x}$  prepared at room temperature for  $x=0, 0.09, 0.16, 0.27, 0.36, 0.46,$  and  $0.55$ . The zero of  $G_{ij}(r)$  for each sample corresponds to  $100x$ .

## B. Electrical resistivity

The electrical resistivity  $\rho$  at 300 K for the samples prepared at room temperature decreases with increasing Cr content as shown in Fig. 4. The decrease in the deposition temperature  $T_D$  results in the increase in  $\rho_{300 \text{ K}}$ , while there is an ambiguity in the composition dependence of  $\rho_{300 \text{ K}}$  for the low- $T_D$  samples owing to insufficient control of  $T_D$  during evaporation.

We review the temperature dependence of  $\rho$  for the amorphous  $\text{Cr}_x\text{Ge}_{1-x}$  in Ref. 7 (Fig. 5):

(1) For  $x=0.05$  and  $0.08$ , a rapid decrease in  $\rho$  with increasing temperature is observed at low temperatures. The relative resistivity  $\rho/\rho_{300 \text{ K}}$  for  $x=0.05$  is larger than that for  $x=0.08$ .

(2) For  $0.17 \leq x \leq 0.45$ , there is a maximum at  $T_{\text{max}}$  which increases with increasing Cr content. The increase in Cr content also results in the decrease in  $\rho(T_{\text{max}})/\rho_{300 \text{ K}}$  and broader shape of the maximum.

(3) For  $x=0.50$ , there are a minimum and a maximum in  $\rho$ - $T$  curve at  $T_{\text{min}}$  and  $T_{\text{max}}$ . In the neighborhood of  $T_{\text{min}}$ , the  $\ln T$  and  $T^2$  dependences are observed below and above  $T=T_{\text{min}}$ , respectively (Fig. 3 in Ref. 7).

(4) For  $x=0.55$  and  $0.65$ ,  $\rho$  shows a monotonic decrease with increasing temperature.

On the other hand, the behavior of  $\rho$  for samples with  $T_D \approx 130 \text{ K}$  is abridged as follows.

(1) For  $x=0.057$  and  $0.088$ , increase in temperature results in a rapid decrease in  $\rho$ . The low-temperature decrease in  $\rho$  for  $x=0.057$  is more rapid than that for  $x=0.088$  [Fig. 6(a)].

(2) For  $x=0.22$ , a monotonic decrease in  $\rho$  is observed with increasing temperature although weakly anomalous behavior occurs at low temperatures [Fig. 6(b)].

(3) For  $x=0.27$  and  $0.32$ , there is a maximum at  $T_{\text{max}}$ . With increasing Cr content, the increase in  $T_{\text{max}}$ , the decrease in  $\rho(T_{\text{max}})/\rho_{300 \text{ K}}$  and the broader shape of the maximum are observed. The low- $T_D$  alloy shows a lower  $T_{\text{max}}$  and a larger  $\rho(T_{\text{max}})/\rho_{300 \text{ K}}$  than those of the high- $T_D$  alloy with the same Cr content. Furthermore, a minimum is observed in a low-temperature range for  $x=0.27$  [Fig. 7(a)].

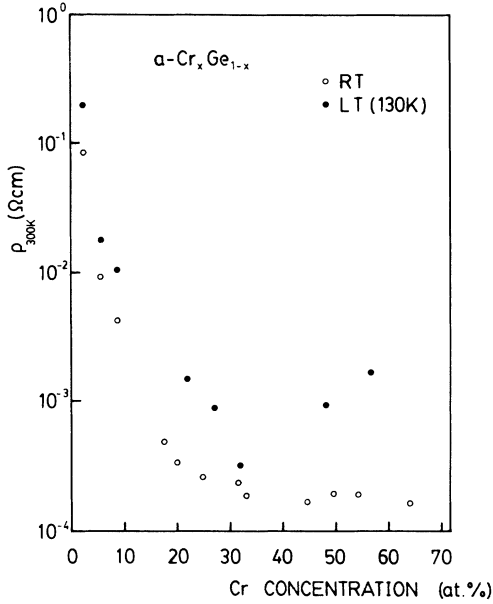


FIG. 4. Electrical resistivity measured at 300 K,  $\rho_{300\text{K}}$ , as a function of Cr fraction  $x$ . Open and solid circles show samples evaporated at room temperature and 130 K, respectively.

(4) For  $x=0.49$  and  $0.57$ ,  $\rho$  shows a monotonic decrease with increasing temperature. The low temperature decrease in  $\rho$  for  $x=0.57$  is more rapid than those of the high- $T_D$  alloys with  $0.55$  and  $0.65$  [Fig. 7(b)].

### C. Magnetic measurements

Figure 8 shows the  $\sigma$ - $H$  plots for several amorphous  $\text{Cr}_x\text{Ge}_{1-x}$  samples prepared at room temperature with  $0.23 \leq x \leq 0.53$  measured at 4.2 K. A linear relation between  $\sigma$  and  $H$  is observed for all samples, suggesting no spontaneous magnetization. The value of  $\sigma$  increases with increasing Cr content, although an opposite relation is observed between those of  $x=0.27$  and  $0.38$ . Here, we must give a brief explanation for the curious aspect for  $x=0.27$  and  $0.38$ . This reversal is not attributed to error

in the magnetization measurement because of its reproducibility. We checked the amorphous nature of samples with  $x$  rays. Furthermore, there were no inhomogeneities in Cr composition in the single sample. A possible explanation for the complex composition dependence of magnetization is made on the basis of differences in the local environment of Cr atoms due to slight differences in preparation conditions, namely, evaporation rate, substrate temperature, and so on. Therefore, it is suggested that the electrical and magnetic properties of the amorphous  $\text{Cr}_x\text{Ge}_{1-x}$  alloys are sensitive to their local environment.

The magnetic susceptibility  $\chi$  for several amorphous  $\text{Cr}_x\text{Ge}_{1-x}$  samples prepared at room temperature with  $0.23 \leq x \leq 0.54$  at 6.3 kOe in Fig. 9 suggests that  $\chi$  consists of the temperature-independent susceptibility  $\chi_0$  and the Curie-Weiss term due to the Cr moment as follows:

$$\chi = \chi_0 + C / (T - \Theta), \quad (1)$$

where  $C = N\mu_{\text{eff}}^2/3k_B$ ,  $N$  is the number of Cr atom per gram of the alloy, and the other symbols have their usual meaning. Then, the susceptibility data could be analyzed by a least-squares fit to Eq. (1), and the parameters  $\chi_0$ ,  $\Theta$ ,  $C$ , and  $\mu_{\text{eff}}$  were determined as shown in Table I. Furthermore, we confirmed the linear relation between  $\Delta\chi^{-1}$  and  $T$  even at low temperatures, as shown in Fig. 10, where  $\Delta\chi = \chi - \chi_0$ . The value of  $\chi_0$  has a tendency to increase with increasing Cr content. The value of  $\Theta$  is negative for  $0.23 \leq x \leq 0.54$  and the absolute value increases with increasing Cr content. On the other hand,  $C$  or  $\mu_{\text{eff}}$  is scarcely dependent on Cr content. The calculated spin  $S$ , assuming  $g=2$ , is more than an order of magnitude smaller than that expected for the  $\text{Cr}^{3+}$  ion ( $S = \frac{3}{2}$ ).

## IV. DISCUSSION

The first and second peaks in  $G_{\text{GeGe}}(r)$  for  $x \leq 0.16$  correspond to the first and second nearest-neighbor atomic distances of crystalline Ge ( $d_1 = 2.44 \text{ \AA}$  and  $d_2 = 4.00 \text{ \AA}$ ), which suggests the tetrahedral random network structure of amorphous  $\text{Cr}_x\text{Ge}_{1-x}$  with small  $x$ . The disappear-

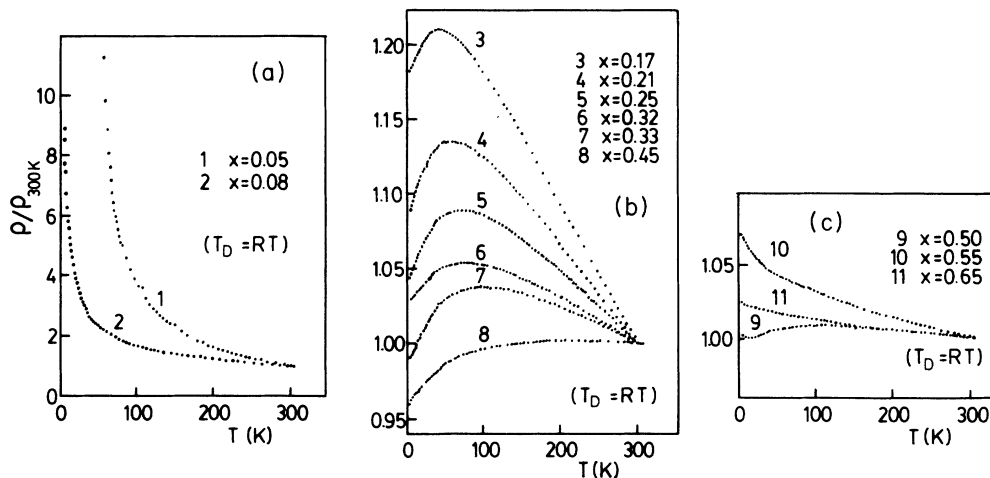


FIG. 5. Temperature dependence of  $\rho/\rho_{300\text{K}}$  for several amorphous  $\text{Cr}_x\text{Ge}_{1-x}$  samples evaporated at room temperature (Ref. 7).

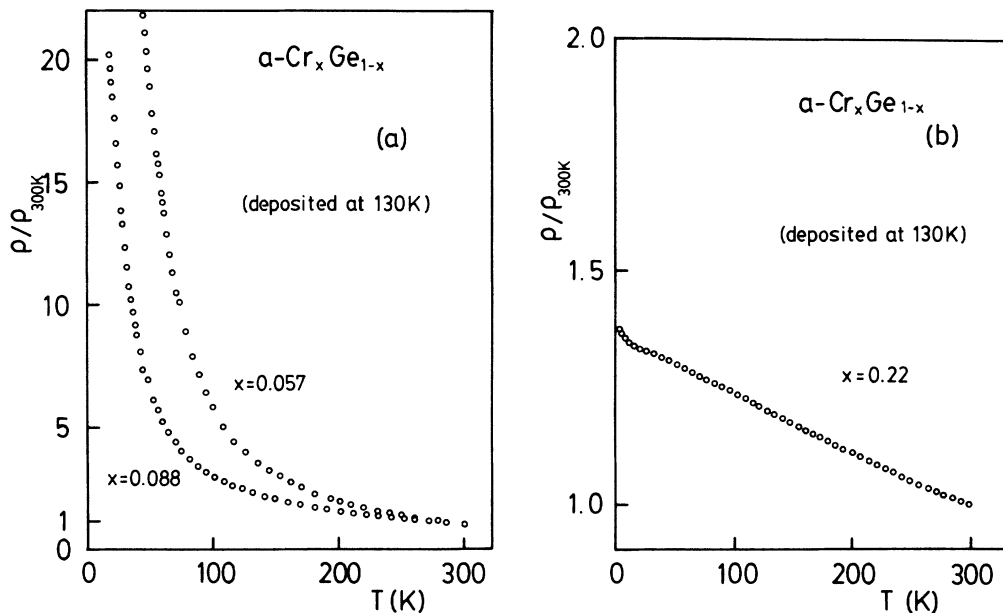


FIG. 6. Temperature dependence of  $\rho/\rho_{300\text{K}}$  for amorphous (a)  $\text{Cr}_{0.057}\text{Ge}_{0.943}$  and  $\text{Cr}_{0.088}\text{Ge}_{0.912}$ , and (b)  $\text{Cr}_{0.22}\text{Ge}_{0.78}$  evaporated at  $T_D = 130\text{K}$ .

ance of the first peak and the shift of the second peak in  $S(K)$  reflect a change in the structure with increasing Cr content. For higher Cr concentration the splitting of the second peak in  $S(K)$  and the appearance of the peak in  $G_{\text{CrCr}}(r)$  centered at  $2\text{Å}$  reflect its amorphous metal-like feature, namely the dense random-packing structure. We can comprehensively mention that the tetrahedral random structure is dominant for  $x \leq 0.16$  while it is replaced by the dense random-packing structure for higher Cr content.

We compare the partial distribution functions of amorphous  $\text{Cr}_{0.37}\text{Ge}_{0.63}$  and  $\text{Cr}_{0.55}\text{Ge}_{0.45}$  with the correspond-

ing atomic distances and coordination numbers of the compounds  $\text{Cr}_{11}\text{Ge}_{19}$  and  $\text{Cr}_{11}\text{Ge}_8$  in Fig. 11, where the position and height of bar represent the atomic distance and coordination number, respectively. We verify the correspondence for Ge-Ge and Cr-Ge pairs between  $G_{ij}(r)$  and the atomic coordination of the crystalline compounds, while the position of the first peak in  $G_{\text{CrCr}}(r)$  does not agree with the corresponding Cr-Cr nearest-neighbor distance. This disagreement suggests the shorter Cr-Cr distance in amorphous alloy with the dense random-packing structure.

The change in the spatial structure is reflected in the

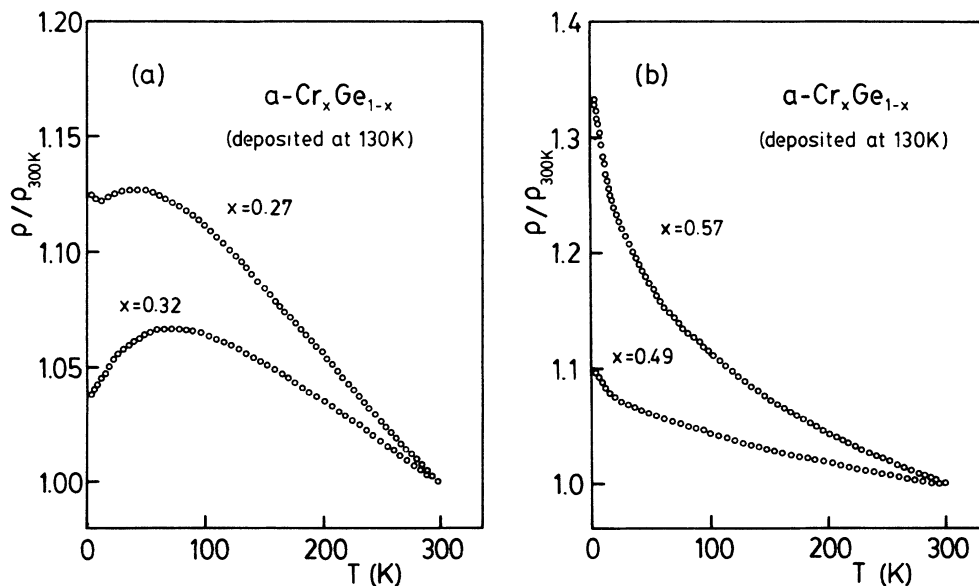


FIG. 7. Temperature dependence of  $\rho/\rho_{300\text{K}}$  for amorphous  $\text{Cr}_x\text{Ge}_{1-x}$  samples for  $x=0.27, 0.32, 0.49,$  and  $0.57$ , evaporated at  $T_D = 130\text{K}$ .

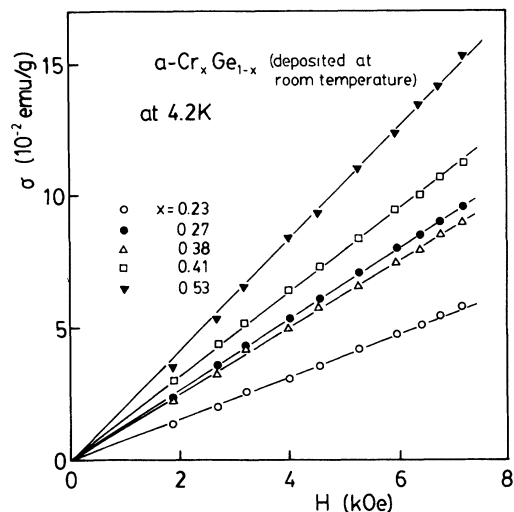


FIG. 8. Magnetization at 4.2 K of several samples of amorphous  $\text{Cr}_x\text{Ge}_{1-x}$  prepared at room temperature.

value of  $\rho_{300\text{ K}}$  and the temperature dependence of  $\rho/\rho_{300\text{ K}}$ . Namely, the tetrahedral random network structure corresponds to large value of  $\rho_{300\text{ K}}$  and the rapid decrease in  $\rho/\rho_{300\text{ K}}$  with increasing temperature, suggesting the semiconductorlike behavior in dilute alloys of amorphous  $\text{Cr}_x\text{Ge}_{1-x}$ . On the other hand, for the concentrated alloy with the dense random packing structure, the scarce concentration dependence of  $\rho_{300\text{ K}}$  and a variety of temperature dependence of  $\rho/\rho_{300\text{ K}}$  are observed.

The decrease in  $T_D$  results in the increase in  $\rho_{300\text{ K}}$  over the whole composition range. This behavior of electrical resistivity can be explained by two kinds of mechanisms: One is a change in the degree of microscopic inhomogeneity, namely microscopic defect structure, and the other is a change in more microscopic spatial structure, with a degree of randomness which should intrinsically affect the structure factor. Hauser and Staudinger<sup>31</sup> found that the amorphous germanium film has a defect structure consisting of a three-dimensional network of density-deficient channels and the electrical properties related to the defect structure. Indeed, the resistivity of the amorphous germanium film deposited at 77 K and annealed at 300 K was larger than that deposited at 300 K.

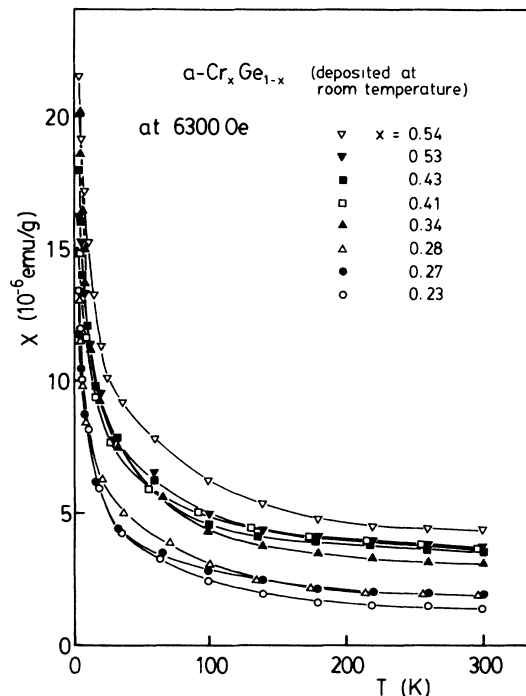


FIG. 9. Magnetic susceptibility at 6300 Oe of several samples of amorphous  $\text{Cr}_x\text{Ge}_{1-x}$  prepared at room temperature.

Then, this idea of defect structure can explain the present behavior of  $\rho_{300\text{ K}}$  in amorphous  $\text{Cr}_x\text{Ge}_{1-x}$  at least in the region having the tetrahedral random structure. On the other hand, lower substrate temperature results in larger values of the effective magneton number per transition-metal atom due to the greater randomness in some amorphous alloys containing transition metals, e.g., amorphous Mn-Zr.<sup>8</sup> This tendency suggests a possibility of change in the microscopic spatial structure with deposition temperature. Although the structure analysis of the low- $T_D$  sample has not been made in the present  $\text{Cr}_x\text{Ge}_{1-x}$  system, it seems safe to speculate that both mechanisms more or less cause the change in  $\rho_{300\text{ K}}$  with  $T_D$ . Furthermore, the concentration dependence of  $\rho(T)/\rho_{300\text{ K}}$  is also affected by the change in  $T_D$ . Then, we have to discuss the feature of  $\rho(T)/\rho_{300\text{ K}}$  in connection with the value of  $\rho_{300\text{ K}}$ .

TABLE I. Parameters obtained from the Curie-Weiss fitting for the amorphous  $\text{Cr}_x\text{Ge}_{1-x}$  susceptibility data.

Cr fraction $x$	$\chi_0$ ( $10^6$ emu/g)	$\Theta$ (K)	$C$ (emu K/mol)	$\mu_{\text{eff}}$ ( $\mu_B$ )	$S$
0.23	1.36	-3.76	0.022	0.42	0.042
0.27	1.86	-4.46	0.017	0.37	0.033
0.28	1.79	-5.53	0.020	0.39	0.037
0.34	2.57	-4.30	0.024	0.44	0.046
0.41	3.61	-5.97	0.016	0.36	0.031
0.43	3.61	-7.98	0.022	0.42	0.042
0.53	3.17	-12.30	0.021	0.43	0.044
0.54	3.79	-9.94	0.023	0.41	0.040

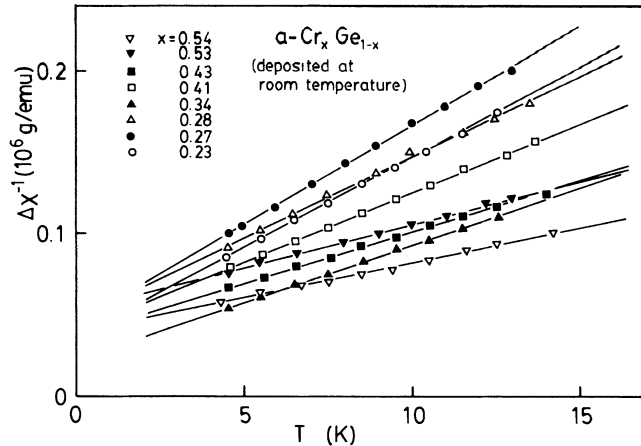


FIG. 10. The inverse susceptibility  $\Delta\chi^{-1}$  as a function of temperature for several samples of amorphous  $\text{Cr}_x\text{Ge}_{1-x}$  prepared at room temperature, where  $\Delta\chi = \chi - \chi_0$  and  $\chi_0$  is the temperature-independent susceptibility.

We can classify the samples into three groups based on the behavior of  $\rho(T)/\rho_{300\text{ K}}$ .

(A) A rapid decrease in  $\rho/\rho_{300\text{ K}}$  is observed at low temperatures:  $x=0.05$  and  $0.08$  for high  $T_D$  and  $x=0.057$  and  $0.088$  for low  $T_D$ .

(B)  $\rho/\rho_{300\text{ K}}$  shows a maximum:  $0.17 \leq x \leq 0.50$  for

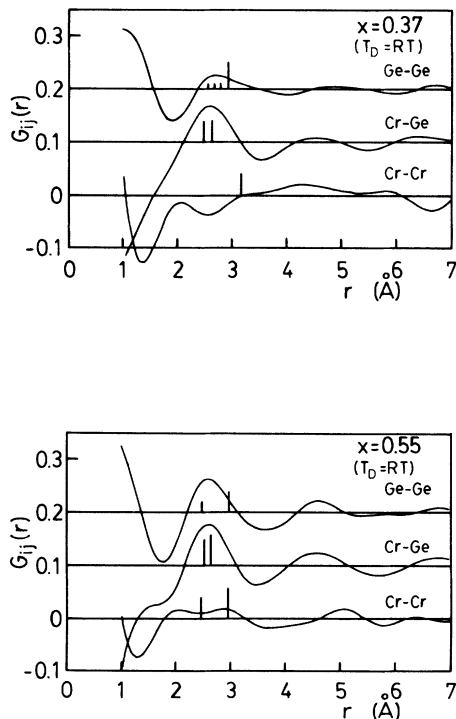


FIG. 11. Comparison of partial pair distribution functions of amorphous  $\text{Cr}_{0.37}\text{Ge}_{0.63}$  and  $\text{Cr}_{0.55}\text{Ge}_{0.45}$  prepared at room temperature with the corresponding atomic distances and coordination numbers of  $\text{Cr}_{11}\text{Ge}_{19}$  and  $\text{Cr}_{11}\text{Ge}_8$ . The positions and heights of bars represent atomic distances and coordination numbers of the crystalline compounds.

high  $T_D$  and  $x=0.27$  and  $0.30$  for low  $T_D$ .

(C) A monotonic decrease in  $\rho/\rho_{300\text{ K}}$  is observed at temperatures below  $300\text{ K}$ :  $x=0.55$  and  $0.65$  for high  $T_D$  and  $x=0.49$  and  $0.57$  for low  $T_D$ .

The rapid decrease in  $\rho$  of sample *A* is characterized by

$$\ln\rho \propto (T_0/T)^{1/4}, \quad (2)$$

except for the high-temperature region near room temperature. We show the relationship for  $x=0.057$  and  $0.088$  with different  $T_D$  in Fig. 12, where we note that the samples with same composition and different  $T_D$  were prepared simultaneously to avoid ambiguity due to error in composition analysis. We also note that the higher resistivity data ( $> 10^5$ ) were eliminated to avoid the error in voltage measurement using a digital multimeter. Mott<sup>32</sup> has predicted the following relation for the temperature  $T_0$  on the basis of his hopping conduction model:

$$T_0 = \lambda\alpha^3/k_B N_F, \quad (3)$$

where  $\alpha$  is the coefficient of exponential decay of the localized states,  $N_F$  is the density of states at the Fermi level, and  $\lambda$  is a dimensionless constant. On the other hand, Ambegaokar *et al.*<sup>33</sup> have shown that consistency of the model requires  $T_0$  to be greater than  $10^6\text{ K}$ . Daver *et al.*<sup>34</sup> measured the electrical resistivity of amorphous  $\text{Cr}_x\text{Ge}_{1-x}$  with  $x \leq 0.135$ , and have indicated the increase in  $N_F$  with increasing Cr content from analysis of  $T_0$ . Furthermore, they estimate that the Cr concentration  $x=0.135$  corresponds to an upper limit of  $N_F$ , above which the overlap of the wave function becomes too large

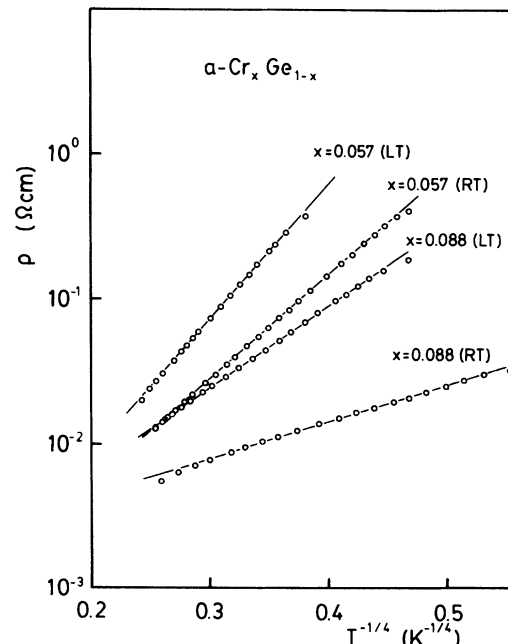


FIG. 12. Electrical resistivity of amorphous  $\text{Cr}_x\text{Ge}_{1-x}$  deposited at room temperature and  $130\text{ K}$  for  $x=0.057$  and  $0.088$  as a function of  $T^{-1/4}$ .

for a localization of levels for the hopping conduction to occur. As shown in Table II, our present data of  $T_0$  are significantly smaller than their values, and do not satisfy Ambegaokar's condition, i.e.,  $T_0 > 10^6$  K. This small  $T_0$  may be caused by other impurities contained in Ge, because pressure during evaporation and evaporation rate do not affect  $T_0$ .<sup>34</sup> However, the present value of  $T_0$  also shows the decrease with increasing Cr content, interpreted as an intrinsic effect, which is consistent with data by Daber *et al.* Furthermore, we are interested in the increase in  $T_0$  with decreasing  $T_D$  in contrast with the trend of amorphous Ge (Ref. 31) and Si-Ge.<sup>35</sup> In the case of amorphous Ge and Si-Ge, the change in  $T_0$  was interpreted in terms of the decrease in  $N_F$  due to the thermal disappearance of disorder with increasing  $T_D$ . If we also interpret the change in  $T_0$  of amorphous  $\text{Cr}_x\text{Ge}_{1-x}$  in terms of Mott's hopping conduction, an increase in  $\alpha$ , namely, a decrease in the length of decay of the localized wave function related to a Cr atom, has to occur as  $T_D$  decreases, since the decrease in  $T_D$  should not cause the decrease in  $N_F$ . This estimation is consistent with an idea of electron localization due to randomness in amorphous materials. Therefore, we claim to support the estimation based on Mott's model for hopping conduction, i.e., the increase in  $N_F$  with increasing Cr content, and the increase in  $\alpha$  with decreasing  $T_D$ . We also note that the critical concentration for semiconductorlike conduction by Daber *et al.*,  $x=0.135$ , is consistent with a tetrahedral random network structure for  $x \leq 0.16$ .

Sample B is accompanied by the disappearance of the tetrahedral random network. The weaker temperature dependence and smaller value of  $\rho_{300\text{ K}}$  suggest its metallic behavior. Since we cannot thoroughly take into consideration about a trace of the structure for sample A, we will tentatively discuss the concentration dependence of  $\rho(T)/\rho_{300\text{ K}}$  on the basis of a theory for amorphous metals. Meisel and Cote<sup>12,13</sup> analyze electrical resistivity in amorphous metals in the context of the Baym-Faber-Ziman theory<sup>36-38</sup> incorporating with electron mean-free-path effects through the Pippard-Ziman condition.<sup>39,40</sup> They calculated the temperature dependence of resistivity as a function of  $2k_F/K_p$  and the mean free path  $\Lambda$ , where  $k_F$  is the Fermi wave number and  $K_p$  is

the scatter vector corresponding to the first peak in  $S(K)$ . We know the substantial constant  $K_p$  from data of  $S(K)$  for  $x > 0.16$ . Furthermore, scarce concentration dependence of  $\rho_{300\text{ K}}$  suggests a value of  $\Lambda$  independent of the Cr content. Therefore, we can roughly analyze the concentration dependence of  $\rho(T)/\rho_{300\text{ K}}$  only in terms of a change in  $k_F$ . Our data for sample B with high  $T_D$  show a shift in  $T_{\text{max}}$  in the direction of high temperature and a broadening of the maximum, namely a decrease in absolute value of the temperature coefficient of resistivity (TCR)  $C_{\text{TCR}}$  with increasing Cr content. Both the features correspond to the increase in  $k_F$  in terms of Ref. 13. The minimum in  $\rho$  observed for a few of samples B can also be explained by the theory, without introducing another extrinsic mechanism. On the other hand, the decrease in  $T_D$  invites the decrease in  $T_{\text{max}}$  and the increase in  $|C_{\text{TCR}}|$ , suggesting a decrease in  $\Lambda$ . This suggestion is consistent with the increase in  $\rho_{300\text{ K}}$  with decreasing  $T_D$ . Furthermore, the change in the temperature coefficient of resistivity can also be expected from the recent analysis taking into consideration the electron localization in a disordered metallic system.<sup>41</sup>

On the other hand, the theory of Ref. 13 cannot give an adequate explanation for the feature of sample C, although an unreasonable assumption may be made in terms of extraordinarily high value of  $T_{\text{max}}$ . We note that the low-temperature behavior is similar to that of an amorphous spin-glass system.<sup>42-45</sup> Therefore, we cannot give a reasonable explanation for the temperature dependence of  $\rho$  for sample C without a detailed discussion of the magnetic properties.

No spontaneous magnetization and the Curie-Weiss-type magnetic susceptibility indicate the paramagnetic properties characterized by localization of Cr moment. Disappearance of the ferromagnetic phase in the amorphous system is qualitatively explained in terms of the decrease in the Cr-Cr nearest-neighbor distance  $d_{\text{Cr-Cr}}$  with amorphization, if we notice the magnetism of crystalline Cr-Ge compounds with changing  $d_{\text{Cr-Cr}}$ .<sup>24,25</sup> On the other hand, the tendency of localizing of moment observed even for high Cr concentration is in contrast to the itinerant-electron-type paramagnetism in the corresponding crystalline compounds. This difference can be inter-

TABLE II. Evaporation conditions and estimated value of  $T_0$  for amorphous  $\text{Cr}_x\text{Ge}_{1-x}$ .

Cr fraction	Initial pressure (Torr)	Pressure during evaporation (Torr)	Substrate temperature $T_D$ (K)	$T_0$ (K)
0.057	$5 \times 10^{-6}$	$1 \times 10^{-5}$	RT	$7.3 \times 10^4$
0.057	$5 \times 10^{-6}$	$1 \times 10^{-5}$	130	$2.1 \times 10^5$
0.088	$5 \times 10^{-6}$	$1 \times 10^{-5}$	RT	$1.1 \times 10^3$
0.088	$5 \times 10^{-6}$	$1 \times 10^5$	130	$2.8 \times 10^4$
0 <sup>a</sup>	$4 \times 10^{-10}$	$4 \times 10^{-10}$	353	$1.47 \times 10^8$
0 <sup>a</sup>	$1 \times 10^{-7}$	$1 \times 10^{-6}$	295	$1.47 \times 10^8$
0.03 <sup>a</sup>	$2 \times 10^{-10}$	$6 \times 10^{-10}$	77	$2.15 \times 10^7$
0.07 <sup>a</sup>	$4 \times 10^{-8}$	$8 \times 10^{-7}$	77	$3.1 \times 10^6$
0.135 <sup>a</sup>	$7 \times 10^{-8}$	$1 \times 10^{-6}$	77	$1.3 \times 10^6$

<sup>a</sup>Data by Daber *et al.*



preted as a difference in localization of  $3d$  electrons of Cr due to the random effects and/or change in the  $3d$ -band structure near  $E_F$  accompanied by a structural change. However, the anomalously small Cr moment estimated for the amorphous  $\text{Cr}_x\text{Ge}_{1-x}$  system is curious although some similar examples have been reported, e.g., a small Fe moment in an amorphous  $\text{Zr}_{40}\text{Cu}_{60-x}\text{Fe}_x$  alloy.<sup>1,3</sup> Two kinds of possible explanation can be done to interpret how such small moment occurs. First, when  $E_F$  is located inside a broad virtual bound  $d$  state with strong  $s$ - $d$  mixing, each Cr atom has a small moment. Second, if a local environment effect stabilizes some of the Cr moments, the average moment becomes small. Considering that the  $\rho(T)$  suggests the monotonic change in  $E_F$  in the amorphous  $\text{Cr}_x\text{Ge}_{1-x}$  system, the moment per Cr atom should change systematically with Cr content. However,  $\mu_{\text{eff}}$  per Cr atom shows scarce concentration dependence, suggesting inadequate explanation of the former. The small moment of Fe in amorphous  $\text{Zr}_{40}\text{Cu}_{60-x}\text{Fe}_x$  alloy has been understood in terms of the retaining of moment only for Fe atoms in certain local environments,<sup>3</sup> e.g., those having at least one Fe atom within nearest neighbors. However, such an interpretation is also inconsistent with the scarce concentration dependence of  $\mu_{\text{eff}}$ , since it must lead to a significant increase in  $\mu_{\text{eff}}$  with increasing Cr content. Therefore, an individual explanation mentioned above is not enough to understand our magnetic data. To realize such dependence of  $\mu_{\text{eff}}$ , there has to be competitive trends so as to suppress the change. Therefore, we propose a model based on the combination of two kinds of explanation as the candidate for the origin of the constant  $\mu_{\text{eff}}$ . If one adopts the picture of the virtual bound state for local moment formation, the magnitude of  $\mu_{\text{eff}}$  depends on the width with the  $s$ - $d$  mixing, the splitting of states with intra-atomic exchange interaction, and the position of  $E_F$ . Ignoring the concentration dependence of the width, Cr content correlates with the intra-atomic exchange interaction through a change in local environment besides  $E_F$ . When the splitting of states and the change of  $E_F$  work competitively with each other,  $\mu_{\text{eff}}$  may be independent of Cr concentration. Thus, an origin of the small localized moment can be estimated qualitatively in terms of the virtual bound states subjected to the local environment effect.

Several papers have indicated a possible spin-glass ordering in amorphous localized moment systems.<sup>9,10</sup> However, there is no evidence of such magnetic order in the amorphous  $\text{Cr}_x\text{Ge}_{1-x}$  with  $x \leq 0.54$ , at least for  $T \geq 4.2$  K. On the other hand, our recent paper<sup>11</sup> showed spin-glass properties in amorphous  $\text{Cr}_{1-x}\text{Mn}_x\text{Ge}$ , whose spin-glass transition temperature decreases with decreasing Mn content and approaches 0 K when  $x$  approaches 0. Therefore, we cannot deny spin-glass phase in samples with  $x > 0.54$ . We can claim that the inexplicable resistivity of the sample C is attributed to the magnetic origin.

Finally, we briefly try to compare the electrical and magnetic properties of amorphous  $\text{Cr}_x\text{Ge}_{1-x}$  with other amorphous alloys containing Ge. First, we pick up the noble-metal germanium alloys, e.g., Ag-Ge (Ref. 46) and Au-Ge (Ref. 47). These alloys show typical temperature

dependence of electrical resistivity of amorphous metal, e.g., typical order of  $C_{\text{TCR}}$ , reasonably explained in terms of the modified Ziman theory,<sup>12,13</sup> because of their non-magnetic properties. However, we should note that Nauyen *et al.*<sup>48</sup> pointed out the invalidity of the rigid-band model in amorphous Au-Ge alloy because of occurrence of the  $sp$ - $d$  hybridization. On the other hand, although the electrical resistivity of amorphous transition-metal-germanium alloys characterized by localized magnetic moment has no adequate theoretical explanation because of the complex scattering mechanisms, the amorphous alloy with comparatively weak interaction between the localized moments such as spin glass often satisfies the following phenomenological equation:<sup>49</sup>

$$\rho(T)/\rho_{300\text{K}} = A + B \exp(-CT), \quad (4)$$

where  $A$ ,  $B$ , and  $C$  are constants characterizing the magnetic properties. We also reported that the electrical resistivity of amorphous  $\text{Cr}_{1-x}\text{Mn}_x\text{Ge}$  satisfies Eq. (4) for  $x \geq 0.3$ ,<sup>45</sup> characterized by spin-glass interaction between localized moment on Mn atoms.<sup>11</sup> In the amorphous  $\text{Cr}_x\text{Ge}_{1-x}$  alloy, temperature dependence of  $\rho$  is more significant than that expected from the modified Ziman theory and is not expressed by Eq. (4) except for the most Cr-concentrated sample. Therefore, it is safe to speculate that the complex behavior of electrical resistivity of amorphous  $\text{Cr}_x\text{Ge}_{1-x}$  is attributed to its intermediate magnetic nature with small localized magnetic moment on Cr atoms.

## V. CONCLUSIONS

Amorphous structure is verified for  $\text{Cr}_x\text{Ge}_{1-x}$  with  $x \leq 0.65$ , changing from the tetrahedral random network to the dense random packing with increasing Cr content. The electrical resistivity shows a change from semiconductorlike conduction characterized in terms of Mott's hopping conduction to the metal-like one in accordance with each amorphous structure. Analysis of electrical resistivity suggests an increase in density of states at the Fermi level in the semiconductor region and an increasing in the Fermi wave number in the metal region with increasing Cr content. As substrate temperature lowers during evaporation, the characterized temperature  $T_0$  increases as well as the electrical resistivity, which suggests a decrease in length of decay of a localized wave function or more localized electron distribution on Cr atoms. The magnetic susceptibility shows Curie-Weiss-like behavior characterized in terms of significantly small localized moment per Cr atom. The small moment is explained on the basis of the idea of the virtual bound state, taking account of the local-environment effect.

## ACKNOWLEDGMENTS

The authors wish to thank Professor S. Anzai of Keio University and Professor I. Kawasumi of Kyorin Univer-

sity for many stimulating discussions. Thanks are also due to Mr. A. Otani for his help during the electrical resistivity measurements. This work was partly supported under a Grant-in-Aid for Scientific Research from the

Ministry of Education, Science and Culture, by the Casio Science Promotion Foundation, and by Takeda Science Foundation.

- \*Present address: Central Research and Development Bureau, Nippon Steel Corporation, 1618 Ida, Nakahara-ku, Kawasaki-shi, Kanagawa 211, Japan.
- <sup>1</sup>F. R. Szofran, G. R. Gruzalski, J. W. Weymouth, D. J. Sellmyer, and B. C. Giessen, *Phys. Rev. B* **14**, 2160 (1976).
  - <sup>2</sup>T. Mizoguchi and T. Kudo, in *Magnetism and Magnetic Materials—1975 (Philadelphia)*, Proceedings of the 21st Annual Conference on Magnetism and Magnetic Materials, AIP Conf. Proc. No. 29, edited by J. J. Becker, G. H. Lander, and J. J. Rhyne (AIP, New York, 1976), p. 167.
  - <sup>3</sup>H. von Lohneysen, G. V. Lecomte, J. Kastner, H. J. Schink, and R. van der Berg, *Phys. Lett.* **98A**, 47 (1983).
  - <sup>4</sup>J. B. Bieri, A. Fert, G. Creuzet, and J. C. Ousset, *Solid State Commun.* **49**, 849 (1984).
  - <sup>5</sup>P. Deppe, K. Fukamichi, F. S. Li, M. Rosenberg, and M. Sostarich, *IEEE Trans. Magn.* **MAG-20**, 1367 (1984).
  - <sup>6</sup>K. M. Unruh and C. L. Chien, *Phys. Rev. B* **30**, 4968 (1984).
  - <sup>7</sup>T. Sato, K. Shimono, K. Iida, A. Jono, E. Ohta, and M. Sakata, *J. Magn. Soc. Jpn.* **8**, 137 (1984).
  - <sup>8</sup>J. J. Hauser and J. V. Waszczak, *Phys. Rev. B* **30**, 2898 (1984).
  - <sup>9</sup>J. J. Hauser, J. V. Waszczak, R. J. Felder, and S. M. Vincent, *Phys. Rev. B* **32**, 7315 (1985).
  - <sup>10</sup>J. J. Hauser, H. S. Chen, G. P. Espinosa, and J. V. Waszczak, *Phys. Rev. B* **34**, 4674 (1986).
  - <sup>11</sup>T. Sato, H. Kamei, T. Nemoto, E. Ohta, M. Sakata, T. Goto, and T. Sakakibara, *J. Phys. F* **18**, 1593 (1988).
  - <sup>12</sup>L. V. Meisel and P. J. Cote, *Phys. Rev. B* **27**, 4617 (1983).
  - <sup>13</sup>L. V. Meisel and P. J. Cote, *Phys. Rev. B* **30**, 1743 (1984).
  - <sup>14</sup>I. G. Fakidov and N. P. Grazhdankina, *Fiz. Met. Metalloved.* **6**, 67 (1958).
  - <sup>15</sup>S. D. Margolin and I. G. Fakidov, *Fiz. Met. Metalloved.* **9**, 823 (1960).
  - <sup>16</sup>H. Vollenkle, A. Wittman, and H. Nowotny, *Mh. Chem.* **95**, 1544 (1964).
  - <sup>17</sup>K. Yasukochi, K. Yamagiwa, Y. Kusawasa, and K. Sekizawa, *J. Phys. Soc. Jpn.* **21**, 557 (1966).
  - <sup>18</sup>V. L. Zagryazhskii, P. V. Gel'd, and A. K. Stol's, *Izv. Vyssh. Ucheb. Zaved. Fiz.* **11**, 46 (1968).
  - <sup>19</sup>B. Rawal and K. P. Gupta, *J. Less-Common Met.* **27**, 65 (1972).
  - <sup>20</sup>S. N. L'vov, O. G. Grechko, and V. N. Bondarev, *Izv. Vyssh. Ucheb. Zaved. Fiz.* **15**, 59 (1972).
  - <sup>21</sup>M. Kolenda, J. Leciejewicz, and A. Szytula, *Phys. Status Solidi B* **57**, K107 (1973).
  - <sup>22</sup>I. N. Frantsevich, E. A. Zhurakovskii, and V. V. Shvaiko, *Ukr. Fiz. Zh.* **21**, 1339 (1976).
  - <sup>23</sup>I. Kawasumi, S. Knoishi, M. Kubota, and M. Sakata, *Jpn. J. Appl. Phys.* **17**, 2173 (1978).
  - <sup>24</sup>M. Kolenda, J. Stoch, and A. Szytula, *J. Magn. Magn. Mater.* **20**, 99 (1980).
  - <sup>25</sup>T. Sato and M. Sakata, *J. Phys. Soc. Jpn.* **52**, 1807 (1983).
  - <sup>26</sup>Yu. V. Kudryavtsev, I. Lezhnenko, E. S. Levin, and Yu. S. Alekseev, *Izv. Akad. Nauk SSSR, Neorg. Mater.* **15**, 220 (1978).
  - <sup>27</sup>Y. Waseda and S. Tamaki, *Z. Phys. B* **23**, 315 (1976).
  - <sup>28</sup>D. T. Cromer and J. T. Waber, *Acta Crystallogr.* **18**, 104 (1965).
  - <sup>29</sup>D. T. Cromer, *Acta Crystallogr.* **18**, 17 (1965).
  - <sup>30</sup>F. G. Edwards, J. E. Enderby, R. A. Howe, and D. I. Page, *J. Phys. C* **8**, 3483 (1975).
  - <sup>31</sup>J. J. Hauser and A. Staudinger, *Phys. Rev. B* **8**, 607 (1973).
  - <sup>32</sup>N. F. Mott, *Philos. Mag.* **19**, 835 (1969).
  - <sup>33</sup>V. Ambegaokar, B. I. Halperin, and J. S. Langer, *Phys. Rev. B* **4**, 2612 (1971).
  - <sup>34</sup>H. Daver, O. Massenet, and B. K. Chakraverty, *Solid State Commun.* **11**, 131 (1972).
  - <sup>35</sup>J. J. Hauser, *Phys. Rev. B* **8**, 3817 (1973).
  - <sup>36</sup>T. E. Faber, *Liquid Metals* (Cambridge University Press, London, 1972).
  - <sup>37</sup>J. M. Ziman, *Philos. Mag.* **6**, 1013 (1961).
  - <sup>38</sup>G. Baym, *Phys. Rev.* **135**, A1691 (1964).
  - <sup>39</sup>J. M. Ziman, *Electron and Phonons* (Clarendon, Oxford, 1960), Chap. 5.
  - <sup>40</sup>A. B. Pippard, *Philos. Mag.* **46**, 1104 (1955).
  - <sup>41</sup>C. C. Tsuei, *Phys. Rev. Lett.* **57**, 1943 (1986).
  - <sup>42</sup>K. V. Rao, T. Egami, H. Gudmundsson, H. U. Astrom, H. S. Chen, and W. Negele, *J. Appl. Phys.* **52**, 2187 (1981).
  - <sup>43</sup>J. J. Hauser, *Solid State Commun.* **30**, 201 (1979).
  - <sup>44</sup>J. J. Hauser, F. S. L. Hsu, G. W. Kammlott, and J. V. Waszczak, *Phys. Rev. B* **20**, 3391 (1979).
  - <sup>45</sup>T. Sato, K. Ikkatai, E. Ohta, and M. Sakata, *J. Phys. F* **14**, 2087 (1984).
  - <sup>46</sup>V. Nguyen Van, S. Fisson, and M. L. Theye, *Thin Solid Films* **89**, 315 (1982).
  - <sup>47</sup>V. Nguyen Van, S. Fisson, and M. L. Theye, *Proceedings of the 8th International Vacuum Congress, Cannes, 1980* (unpublished).
  - <sup>48</sup>V. Nguyen Van, M. L. Theye, and S. Fission, *J. Phys. (Paris), Colloq.* **41**, C8-489 (1980).
  - <sup>49</sup>H. Gudmundsson, H. U. Astrom, D. New, K. V. Rao, and H. S. Chen, *J. Phys. (Paris), Colloq.* **39**, C6-943 (1978).